Acceleration of Age-Related Changes in the Retina in α-Tocopherol Transfer Protein Null Mice Fed a Vitamin E–Deficient Diet

Masaki Tanito,[1] *Yasukazu Yoshida,*[2] *Sachiko Kaidzu,*[1] *Zhi-Hua Chen,*[2] *Osamu Cynshi,*[3] *Kou-ichi Jishage,*[3] *Etsuo Niki,*[2] *and Akihiro Ohira*[1]

Purpose. To assess the role of vitamin E (VE) in age-related changes in the retinal tissues by using a mouse model of severe VE deficiency.

Methods. Pups of α-tocopherol transfer protein null (*a-TTP*$^{-/-}$) mice were fed a VE-deficient diet for 4 or 18 months (VE (−) group). Wild-type C57BL/6 mice were fed a 0.002% α-tocopherol–supplemented diet (VE (+) group). In various ocular tissues, the VE levels were measured by high-performance liquid chromatography; the fatty acid composition by gas chromatography (GC); and the hydroxyoctadecadienoic acid and 8-iso-prostaglandin $F_{2\alpha}$ levels, which are biomarkers for lipid peroxidation, by GC-mass spectrometry. The retinal structure was assessed by light, electron, and fluorescence microscopy.

Results. The α-tocopherol level in the retinas obtained from 4-month-old VE (−) animals was 71-fold lower than that in the retinas obtained from the VE (+) group. In addition, γ-tocopherol was not detected; thus, the VE (−) group demonstrated a more severe VE deficiency than ever reported. In this group, the concentration of n-3 polyunsaturated fatty acids decreased (0.3- to 0.9-fold), whereas that of other classes of fatty acids was unchanged or increased. At 18 months of age, the number of the outer nuclear layer (ONL) nuclei was observed to be 17% lower in the VE (−) than in the VE (+) group ($P < 0.05$). Electron microscopy revealed larger amounts of matrix between the ONL nuclei indicating the Müller cell hypertrophy, greatly expanded rod outer segment discs, and a larger number of inclusion bodies in the retinal pigment epithelium (RPE; $P < 0.05$) in the VE (−) group. Fluorescence microscopy revealed that the autofluorescence signal was increased in the RPE layer in this group. When the observations of the 18-month-old animals were compared to those of the 4-month-old animals, the hydroxyoctadecadienoic acid and 8-iso-prostaglandin $F_{2\alpha}$ levels were found to be increased in the retina and RPE obtained from both the VE (−) and VE (+) groups; however, the age-related increases were more remarkable in the VE (−) group (2.6- to 43.5-fold) than in the VE (+) group (0.8- to 8.7-fold).

Conclusions. The combined use of *a-TTP*$^{-/-}$ mice and a VE-deficient diet leads to a severe deficiency of VE, enhances lipid peroxidation in the retina, and accelerates degenerative damage of the retina with age. (*Invest Ophthalmol Vis Sci.* 2007; 48:396–404) DOI:10.1167/iovs.06-0872

There are increasing experimental and clinical evidences that suggest the involvement of the oxidative stress induced by active oxygen and nitrogen species in the pathogenesis of various diseases such as cancer and aging.[1] As a consequence, the role of antioxidants has received much attention.[2] Protection against oxidative stress in ocular tissues is thought to be mediated by several antioxidants, such as the vitamins C and E,[3,4] catalase,[3] superoxide dismutases,[3] the glutathione system,[5,6] and the thioredoxin system.[5,7] Until now, the preventive and therapeutic effects of vitamin E (VE) administration have been reported in various types of human ocular diseases.[8–13]

VE is a generic description for all tocopherol (Toc) and tocotrienol derivatives. Tocopherols have a phytyl chain, while tocotrienols have a similar chain but with three double bonds at positions 3′, 7′, and 11′. Both tocopherols and tocotrienols have four isomers (designated as α, β, γ, and δ), which differ in the number and position of methyl groups on the chroman ring (Supplementary Fig. S1, online at http://www.iovs.org/cgi/content/full/48/1/396/DC1).[14] α-Toc is the most abundant VE in vivo,[15] although plants and normal diets often contain a nearly equal or a higher amount of γ-Toc. α-Toc transfer protein (α-TTP), a cytosolic liver protein with a highly specific binding affinity for α-Toc, selectively transports α-Toc from the liver to the blood stream[16]; thus, the presence of α-TTP is thought to be the reason for such a high bioavailability of α-Toc in vivo. It has been demonstrated that mutations in the gene that encodes α-TTP in humans cause ataxia with isolated VE deficiency (AVED)[17] and autosomal recessive retinitis pigmentosa.[18]

In experimental settings, the role of VE in ocular homeostasis was analyzed after the dietary deprivation of VE in animals.[19–21] However, any attempt to reduce the VE level in ocular tissues was met with some resistance. The concentration of α-Toc was 560 and 120 μg/g tissue in the rat retina after 16 weeks of feeding them regular laboratory chow and a VE-deficient diet, respectively.[19] Further, in the rats fed a VE-deficient diet, there was a roughly 24-, 5-, and 8-fold decrease in the concentration of α-Toc in the iris, whole retina, and retinal pigment epithelium (RPE), respectively, when compared with those fed a regular diet for 15 weeks after weaning.[21] More recently, a mouse with a targeted disruption of the *a-TTP* gene was generated.[22] We recently reported that the concentration of α-Toc in wild-type mice fed a regular diet and *a-TTP*$^{-/-}$ mice maintained on a VE-deficient diet was respectively 2100 and 6 nM in the plasma (a 350-fold decrease) and

From the [1]Department of Ophthalmology, Shimane University School of Medicine, Shimane, Japan; [2]Human Stress Signal Research Center, National Institute of Advanced Industrial Science and Technology (AIST), Osaka, Japan; and [3]Fujigotemba Research Laboratories, Chugai Pharmaceutical Co. Ltd., Shizuoka, Japan.

Supported in part by Grant-in-Aid for Scientific Research (C), 17500495-2005 and 18591921-2006, from the Ministry of Education, Science, Sports and Culture, Japan.

Submitted for publication July 27, 2006; revised September 11 and 27, 2006; accepted November 20, 2006.

Disclosure: **M. Tanito**, None; **Y. Yoshida**, None; **S. Kaidzu**, None; **Z.-H. Chen**, None; **O. Cynshi**, None; **K.-i. Jishage**, None; **E. Niki**, None; **A. Ohira**, None

The publication costs of this article were defrayed in part by page charge payment. This article must therefore be marked "*advertisement*" in accordance with 18 U.S.C. §1734 solely to indicate this fact.

Corresponding author: Yasukazu Yoshida, Human Stress Signal Research Center (HSSRC), National Institute of Advanced Industrial Science and Technology (AIST), 1-8-31 Midorigaoka, Ikeda, Osaka 563-8577, Japan; yoshida-ya@aist.go.jp.

19.9 and 0.26 nanomoles/g tissue in the liver (a 77-fold decrease) at the age of 11 weeks.[23] Thus, the combined use of *a-TTP*$^{-/-}$ mice and a VE-deficient diet leads to a more severe VE deficiency than ever reported and is thought to be an excellent model to assess the role of VE in vivo.

A previous study indicated that the dietary deprivation of VE and other antioxidants alters the retinal structure through events such as the mild loss of photoreceptor cells,[24] an increase in lipofuscin accumulation in the RPE[19,25] as well as an increase in lipid peroxidation,[26] and a change in the fatty acid composition in rod outer segments (ROS).[20] We recently reported that the totally assessed hydroxyoctadecadienoic acid (tHODE) and 8-iso-prostaglandin $F_{2\alpha}$ (8-iso-$PGF_{2\alpha}$), which are derived from linoleic acid and arachidonic acid, respectively, could be biomarkers for the peroxidation levels in mouse retina.[27] In the present study, we used a model of severe VE deficiency to assess the role of VE in age-related changes in ocular tissues in vivo, particularly in the retina and RPE. For this purpose, the concentration of α- and γ-Toc, the composition of fatty acids in various ocular tissues, and the tHODE and 8-iso-$PGF_{2\alpha}$ levels in the retina and RPE were measured by high-performance liquid chromatography (HPLC) and gas chromatography (GC). In addition, the retinal structure was assessed by light, electron, and fluorescence microscopy in young (4-month-old) and/or old (18-month-old) *a-TTP*$^{-/-}$ mice maintained on a VE-deficient diet and compared to that of the age-matched wild-type mice.

Materials and Methods

Animal Care

All procedures were performed according to the ARVO Statement for the Use of Animals in Ophthalmic and Vision Research. All protocols were reviewed and approved by the Institutional Animal Care and Use Committee (IACUC) of the National Institute of Advanced Industrial Science and Technology. Male *a-TTP*$^{-/-}$ mice (B6.129S7 α-Ttp^{tm1Csk}; 19–24 g)[22] obtained from an in-house colony were fed a VE-free diet (Funabashi Nojyo, Chiba, Japan) during the experimental periods (VE (−) group).[23] Wild-type C57BL/6J mice (19–24 g) were purchased from Nippon Clea Co. (Tokyo, Japan) and were fed the same diet as that fed the VE (−) animals except that it was supplemented with 0.002% (wt/wt) α-Toc (VE (+) group). All animals were maintained until they were 4 or 18 months old under standardized conditions of light (7 AM on/7 PM off; 20–40 lux within the cages during the light cycle), temperature (22°C), and humidity (70%).

Preparation of Ocular Tissue Samples

The preparation of ocular tissue samples has been described previously.[15,27] Briefly, after a deep anesthesia was induced by an intraperitoneal injection of pentobarbital sodium (30 mg/kg), the mice were perfused with ice-cold phosphate-buffered saline (PBS; pH 7.4) from the left ventricle to wash out the blood; subsequently, the eyes were rapidly enucleated. For morphologic analyses, the enucleated eyes were immersed in fixatives, as described in later sections. For the measurements of VE, fatty acid, tHODE, and 8-iso-$PGF_{2\alpha}$, the enucleated eyes were dissected under a microscope into the cornea, crystalline lens, iris, neural retina, and the RPE fraction consisting of the RPE, choroid, and sclera.[15] The right eyes were used for the analyses of VE or the morphology, and the left eyes were used for the analyses of fatty acids or tHODE and 8-iso-$PGF_{2\alpha}$.

Analysis of VE in Ocular Tissues

The method for the analysis of VE was reported previously.[15] The ocular tissues from the 4-month-old animals were homogenized with 100 μL PBS by using pestles and tubes (Bel-Art Products, Pequannock, NJ) for 4 minutes. The protein concentration of the sample was determined using 5 μL of the aliquot and the bicinchoninic acid (BCA) protein assay kit (Pierce, Rockford, IL). Chloroform-methanol (450 μL, 2:1 [vol/vol]) was added to the homogenized suspension, and VE was extracted by centrifugation (15,000*g*, 4°C, 20 minutes) after it was mixed vigorously with a vortex mixer. α-Toc and γ-Toc were separated on a column (5 μm, 250 × 4.6 mm; LC-18 ODSl Sigma-Aldrich Co., Tokyo, Japan) by using methanol/*tert*-butyl alcohol (95:5 [vol/vol]) containing 50 mM sodium perchlorate as the eluent at a flow rate of 1 mL/min. They were detected using an HPLC unit with an amperometric electrochemical detector (Nanospace SI-1; Shiseido, Tokyo, Japan) that was set at 800 mV. The concentrations of VE were determined using the standard samples of α- and γ-Toc (purity, 99.9 wt%) that were kindly provided by Eisai Co., Ltd. (Tokyo, Japan).

Analysis of Fatty Acids in Ocular Tissues

The method for the analysis of fatty acids was reported previously.[23] Lipids were extracted from the ocular tissues of 4-month-old animals in the same manner as described for the VE analysis. An aliquot of the solution containing lipids was evaporated, and methanol/benzene 2 mL (4:1 [vol/vol]) containing an internal standard—tridecanoic acid (600 μg)—was added to it. Acetyl chloride (200 μL) was added slowly to this solution and subjected to methanolysis at 100°C for 1 hour. After the sample was cooled in water, 5 mL of potassium carbonate (6% in water) was added slowly to terminate the reaction and neutralize the mixture. The solution was mixed vigorously with a vortex mixer and centrifuged (3000*g*, 10 minutes), and an aliquot of the benzene layer was injected into a gas chromatograph (GC 6890 N; Agilent Technologies Co., Ltd., Palo Alto, CA) equipped with a flame-ionized detector. A fused-silica capillary column (SP-2560, 100 m × 0.25 mm; Sigma-Aldrich Co.) was used for the analysis. Helium was used as the carrier gas at a flow rate of 1.2 mL/min. The temperature programming was performed from 140°C to 240°C at 4°C/minute. The injector temperature was set at 250°C. The fatty acid composition was expressed as mol% of the total fatty acids.

Analyses of tHODE and 8-iso-$PGF_{2\alpha}$

8-iso-Prostaglandin $F_{2\alpha}$-d_4 [8-iso-$PGF_{2\alpha}$-d_4], 9-hydroxy-10(*E*),12(*Z*)-octadecadienoic acid [9-(*E,Z*)-HODE], 13-hydroxy-9(*Z*),11(*E*)-octadecadienoic acid [13-(*Z,E*)-HODE], and 9(*S*)-hydroxy-10(*E*),12(*Z*)-octadecadienoic-9,10,12,13-d_4 acid [9-HODE-d_4] were obtained from Cayman Chemical Company (Ann Arbor, MI). 9-Hydroxy-10(*E*),12(*E*)-octadecadienoic acid [9-(*E,E*)-HODE] and 13-hydroxy-9(*E*),11(*E*)-octadecadienoic acid [13-(*E,E*)-HODE) were obtained from Larodan Fine Chemicals AB (Malmo, Sweden). The method for the analysis of tHODE and 8-iso-$PGF_{2\alpha}$ has been reported.[27,28] The lipids were extracted from the retinas and RPE fractions of the 4- and 18-month-old animals in same manner as in the VE analysis. The internal standards—8-iso-$PGF_{2\alpha}$-d_4 (100 ng) and 9-HODE-d_4 (100 ng)—and 1 mL of methanol containing 100 μM 2,6-di-*tert*-butyl-4-methylphenol (BHT) were added to the sample, followed by the reduction of hydroperoxides and ketones with an excessive amount of sodium borohydride at room temperature for 5 minutes. The reduced sample was then mixed with 1 M KOH in methanol (1 mL) under nitrogen and incubated for 30 minutes in the dark at 40°C on a shaker. The sample was centrifuged (3000*g*, 4°C, 10 minutes). The supernatant obtained was diluted with a fourfold volume of water (pH 3), and its pH was adjusted to 3 with 2 N HCl. The acidified sample was centrifuged (3000*g*, 4°C, 10 minutes), and the supernatant was subjected to solid phase extraction.[27,28] The eluent obtained was evaporated under nitrogen, and 30 μL of the silylating agent *N,O*-bis(trimethylsilyl)-trifluoroacetamide (BSTFA) was added to the dried residue. The solution was vigorously mixed by vortexing for 1 minute and incubated for 60 minutes at 60°C to obtain trimethylsilyl esters and ethers. An aliquot of this sample was injected into a gas chromatograph (GC 6890 N) equipped with a quadrupole mass spectrometer (5973 Network; Agilent Technologies, Palo Alto, CA). A fused-silica capillary column (HP-5MS, 5% phenyl methyl siloxane, 30 m × 0.25 mm; Agilent Technologies) was used. Helium was used as the carrier gas at a flow rate of 1.2 mL/min. The temperature program-

ming was performed from 60°C to 280°C at 10°C/min. The injector temperature was set at 250°C; the temperatures of the transfer line to the mass detector and the ion source were 250°C and 230°C, respectively. The electron energy was set at 70 eV. On the basis of their retention times and characteristic fragments, 8-iso-$PGF_{2\alpha}$ and each class of HODE were identified (m/z = 571 and 481 for 8-iso-$PGF_{2\alpha}$ and 440, 369, and 225 for HODE; Figs. 1A, 1B). The retinal concentrations of 8-iso-$PGF_{2\alpha}$ and HODE were determined using the fragment ions with an m/z ratio of 481 and 440, respectively. For the quantification of 8-iso-$PGF_{2\alpha}$ and HODE, 8-iso-$PGF_{2\alpha}$-d_4 (*m/z* = 485), and 9-HODE-d_4 (m/z = 444) were used as internal standards, respectively. The values obtained were compared between the VE (−) and VE (+) groups or between the groups comprising 4- and 18-month-old mice by an unpaired *t*-test.

Preparation of Retinal Tissue Sections

For epoxy resin embedding, the right eyes enucleated from the 18-month-old animals were fixed with 2% paraformaldehyde and 2% glutaraldehyde in 0.1 M phosphate buffer (pH 7.4) for 48 hours at 4°C. Subsequently, the cornea and lens were removed from the eyeballs, and the eye cups were radially cut into six pieces. These pieces were postfixed with 2% osmium tetroxide for 2 hours, dehydrated in a graded series of ethanol, and embedded in epoxy resin. For light microscopy, each of the six pieces obtained from each eye was cut into semithin sections (approximately 900 nm thick) and stained with toluidine blue. For electron microscopy, each of the six pieces was cut into ultrathin sections (approximately 90 nm thick) and stained with uranyl acetate and lead citrate. For paraffin embedding, the right eyes enucleated from the 4-month-old animals were fixed with 4% paraformaldehyde and 0.25% glutaraldehyde in PBS for 24 hours at 4°C. Subsequently, the eyes were dehydrated in a graded series of ethanol, embedded in paraffin, and cut into 5-μm-thick sagittal sections, including the optic nerve head.

Light Microscopy

For each eye, digitized color images of six semithin retinal sections of six pieces of retinal block were obtained using a digital imaging system (PDMC Ie; Olympus, Tokyo, Japan). Each image located retinal areas 0.25 to 1 mm away from the optic disc. The thicknesses of the retina, the outer nuclear layer (ONL), and the ROS were measured at the center of each image by using ImageJ 1.32j software (available at http://rsb.info.nih.gov/ij/; developed by Wayne Rasband, National Institutes of Health, Bethesda, MD),[29] and the number of toluidine blue-positive photoreceptor cell nuclei in each image was counted manually.[7,30] The averages of the values obtained for the six sections of each eye were calculated for both VE (−) and VE (+) groups and compared by unpaired *t*-test.

Transmission Electron Microscopy

In each of the six pieces of retinal block obtained from each eye, black and white images were obtained in 4–8 locations, including the inner and outer regions of the retinal layers, RPE, and choroid; the photographs were obtained using a transmission electron microscope (EM-002B; Topcon, Tokyo, Japan) with magnifications between 2200× and 6600×.[31] For the quantification of the number of inclusion bodies in the RPE, the images of the RPE layer located roughly 0.5 mm away from the optic disc were photographed with a magnification of 2200×, and the number of inclusion bodies in each image was counted manually. Six images of the six retinal blocks were counted in each eye. The averages of the values obtained from the six images in each eye were

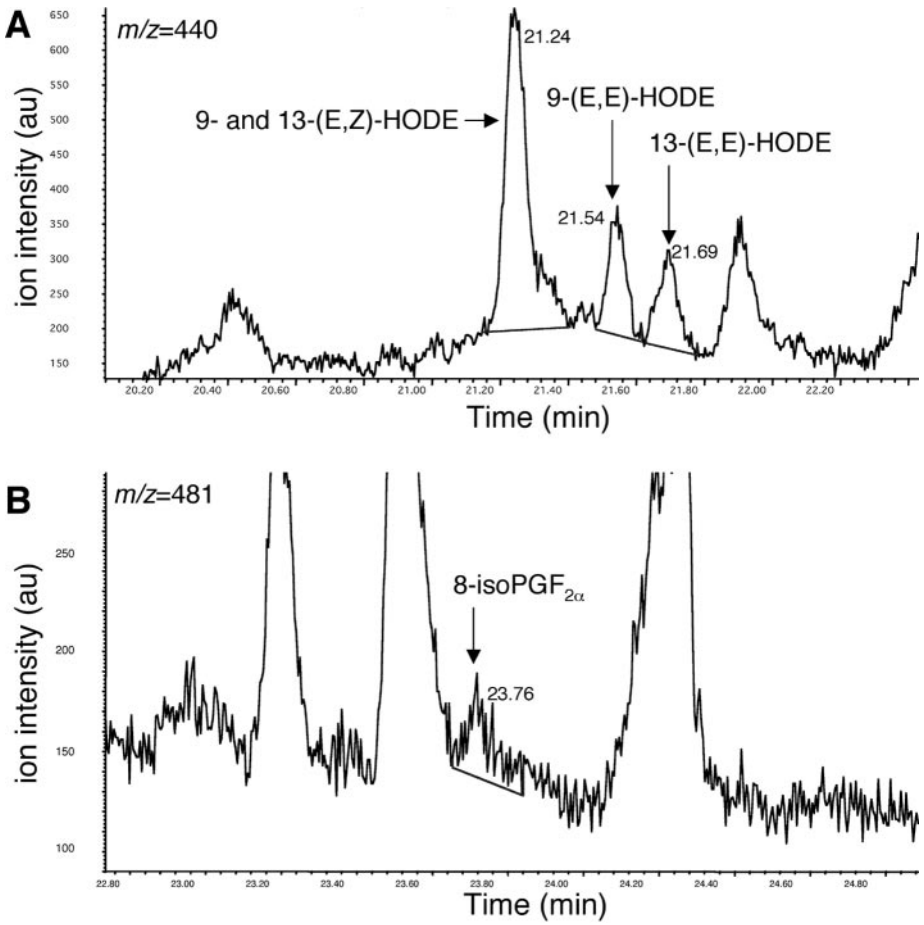

FIGURE 1. Typical GC-MS spectra of the trimethylsilyl ester and ether of HODE (**A**) and 8-iso-$PGF_{2\alpha}$ (**B**) in mouse retina. (*A*) Detected peaks of 9- and 13-(*Z,E*)-HODE, 9-(*E,E*)-HODE, and 13-(*E,E*)-HODE. (**B**) Detected peak of 8-iso-$PGF_{2\alpha}$.

calculated for both VE (−) and VE (+) groups and compared using an unpaired *t*-test.

Fluorescence Microscopy

Autofluorescence from the retinal tissues was detected in the paraffin-embedded sections by using a fluorescence microscope equipped with 494-nm/530-nm excitation/emission filters (IX-71; Olympus).

Results

VE Concentrations in Ocular Tissues

Initially, we tested the VE level in the ocular tissues obtained from the 4-month-old VE (−) and VE (+) animals (Table 1). In the VE (+) group, α-Toc was detected in all the tissues that were analyzed, whereas γ-Toc was detected in the iris, retina, and RPE fraction (Table 1, VE (+)). Both α- and γ-Toc levels were the highest in the retina among the ocular tissues in the VE (+) group; this result was consistent with that described in our previous report on rats.[15] In the VE (−) group, α-Toc was detected in the cornea and retina, and γ-Toc was not detected in any of the tissues (Table 1, VE (−)). The ratio of the VE level (VE (−)/VE (+)) did not exceed 0.1 in any tissue; thus, VE was severely depleted in the ocular tissues obtained from the VE (−) group. Notably, the α-Toc level in the retinas obtained from the VE (+) group was 71-fold lower than those obtained from the VE (−) group.

Fatty Acid Composition in Ocular Tissues

Because age and antioxidant levels affect fatty acid composition,[20,32] we next tested the fatty acid composition in the ocular tissues obtained from the 4-month-old mice from the VE (−) and VE (+) groups (Table 2). In both groups, the fatty acid concentration was below the quantification level in the cornea (Table 2). Unlike the results obtained for other ocular tissues, docosahexaenoic acid (*n*-3 polyunsaturated fatty acid [PUFA]) was found to be the most abundant fatty acid in the retina in both groups (Table 2, retina); this finding was consistent with that described in a previous report.[33,34] In the VE (−) group, the concentration of the n-3 PUFAs decreased consistently in all ocular tissues other than the cornea when compared to the VE (+) group (0.3- to 0.9-fold). In contrast, that of the other kinds of fatty acids such as saturated fatty acids (SFAs), monounsaturated fatty acids (MUFAs) and n-6 PUFAs was unchanged or increased in the VE (−) group in most of the tissues that were analyzed (Table 2). Thus, VE deficiency altered the fatty acid composition in the ocular tissues during the early phase of the experiments.

Light Microscopic Observation

The toluidine blue–stained semithin sections of retinas obtained from the 18-month-old animals were observed by light microscopy (Fig. 2). In the ONL in the VE (−) group, the cellular density was lower, and the intensity of the toluidine blue staining in the ROS adjacent to the RPE was lower than that observed in the VE (+) group (Fig. 2B). Quantification revealed that there was no significant difference in the thicknesses of the total retina, ONL, and ROS of the VE (+) and VE (−) groups (Fig. 2C); however, the number of ONL nuclei was significantly lower in the VE (−) group than in the VE (+) group (17% lower, $P < 0.05$; Fig. 2D). In the VE (−) group, isolated cell nuclei were observed in the outer part of the inner nuclear layer (Fig. 2B, arrows), indicting somatic translocation of Müller cells.[35]

Table 1. Level of Vitamin E in Ocular Tissues from 4-Month-Old animals

	Cornea			Iris			Lens			Retina			RPE Fraction		
	VE(+)	VE(−)	Ratio [VE(−)/(+)]	VE(+)	VE(−)	Ratio [VE(−)/(+)]	VE(+)	VE(−)	Ratio [VE(−)/(+)]	VE(+)	VE(−)	Ratio [VE(−)/(+)]	VE(+)	VE(−)	Ratio [VE(−)/(+)]
α-Toc	27 ± 5	2 ± 3	0.1	85 ± 9	ND	0.0	6 ± 3	ND	0.0	779 ± 127	11 ± 10	0.0	159 ± 12	ND	0.0
γ-Toc	ND	ND	—	21 ± 13	ND	0.0	ND	ND	—	127 ± 41	ND	0.0	30 ± 0	ND	0.0

All values are expressed as mean ± SD (picomoles/mg protein; $n = 4$ in each group).

TABLE 2. Fatty Acid Composition in Ocular Tissues from 4-Month-Old Animals

	Cornea			Iris			Lens			Retina			RPE Fraction		
	VE(+)	VE(−)	Ratio [VE(−)/(+)]	VE(+)	VE(−)	Ratio [VE(−)/(+)]	VE(+)	VE(−)	Ratio [VE(−)/(+)]	VE(+)	VE(−)	Ratio [VE(−)/(+)]	VE(+)	VE(−)	Ratio [VE(−)/(+)]
Saturated															
16:0 (Palmitic acid)	ND	ND	—	15.3	23.9	1.6	21.8	25.1	1.2	21.3	22.0	1.0	20.4	23.7	1.2
18:0 (Stearic acid)	ND	ND	—	17.6	21.3	1.2	17.4	17.6	1.0	19.4	23.3	1.2	22.0	19.0	0.9
Monounsaturated															
16:1 (Palmitoleic acid)	ND	ND	—	4.4	4.5	1.0	4.5	4.7	1.0	1.6	3.5	2.2	4.2	5.0	1.2
18:1 (Oleic acid)	ND	ND	—	9.1	11.1	1.2	20.5	24.9	1.2	10.4	11.7	1.1	10.5	14.2	1.4
Polyunsaturated, n-3															
18:3 (Linolenic acid)	ND	ND	—	17.3	10.0	0.6	13.7	9.3	0.7	5.3	2.6	0.5	12.2	8.4	0.7
22:6 (Docosahexanoic acid)	ND	ND	—	18.0	5.1	0.3	7.7	6.9	0.9	32.1	25.1	0.8	9.6	6.6	0.7
Polyunsaturated, n-6															
18:2 (Linoleic acid)	ND	ND	—	8.9	8.1	0.9	7.6	7.5	1.0	3.5	2.5	0.7	13.5	13.1	1.0
20:4 (Arachidonic acid)	ND	ND	—	9.4	16.1	1.7	6.7	4.0	0.6	6.4	9.4	1.5	7.6	9.9	1.3

All values are expressed as mol% in samples ($n = 4$ in each group). ND, not detectable.

FIGURE 2. Light microscopic observation. The eyes obtained from 18-month-old mice belonging to the VE (+) group (four eyes from four mice) and the VE (−) group (six eyes from six mice) were analyzed. (**A**, **B**) Representative images of toluidine blue–stained semithin retinal sections of the VE (+; **A**) and VE (−; **B**) groups. Isolated cell nuclei were observed in the outer part of the of the inner nuclear layer in the sections obtained from the VE (−) group (*white arrow*). (**C**) Quantifications of the total, ONL, and ROS thicknesses. The data are expressed as the mean ± SD ($n = 4$ and 6 in the VE (+) and VE (−) groups, respectively). NS indicates that there are no significant differences between the VE (−) and VE (+) groups, as determined by an unpaired *t*-test. (**D**) Quantifications of the number of nuclei in the ONL. The data are expressed as the mean ± SD [$n = 4$ and 6 in the VE (+) and VE (−) groups, respectively]. $^*P < 0.05$, as determined by an unpaired *t*-test. INL, inner nuclear layer; ONL, outer nuclear layer; RIS, rod inner segment; ROS, rod outer segment; and RPE, retinal pigment epithelium.

Ultrastructural Observation

We further assessed the ultrastructure of the retina and RPE by TEM in the 18-month-old animals (Fig. 3). In the VE (+) group, the photoreceptor cell nuclei in the ONL were arranged regularly, and a thin layer of matrix filled the spaces between the nuclei (Fig. 3A). In the VE (−) group, the arrangement of the photoreceptor cells was irregular, and a larger amount of matrix filled the spaces between nuclei when compared to the VE (+) group (Fig. 3B, arrows). In the VE (+) group, the disc membranes of the ROS were arranged regularly and densely from the base to the tip of the ROS (Fig. 3C). In the VE (−) animals, the arrangement of the disc membranes at the base of the ROS was relatively uniform and became greatly expanded and irregular at the tip of the ROS (Fig. 3D, arrowheads). In the RPE cells, we observed inclusion bodies that contained whorls of electron dense, membranelike matter (Fig. 3E, arrowheads), some of them being more compressed and electron dense (Fig. 3E, arrow). However, they were distinguishable from melanosomes, which were the most electron dense, completely amorphous, and oval-shaped structures located in both the RPE and choroid (Figs. 3E, 3F, asterisks). Although the inclusion bodies were observed in both groups of animals, more accumulated in the RPE cells in the VE (−) group (Fig. 3H) than in in the VE (+) group (Fig. 3G). Furthermore, quantification revealed that the number of inclusion bodies was significantly larger in the VE (−) group than in the VE (+) group ($P < 0.05$, Fig. 3I).

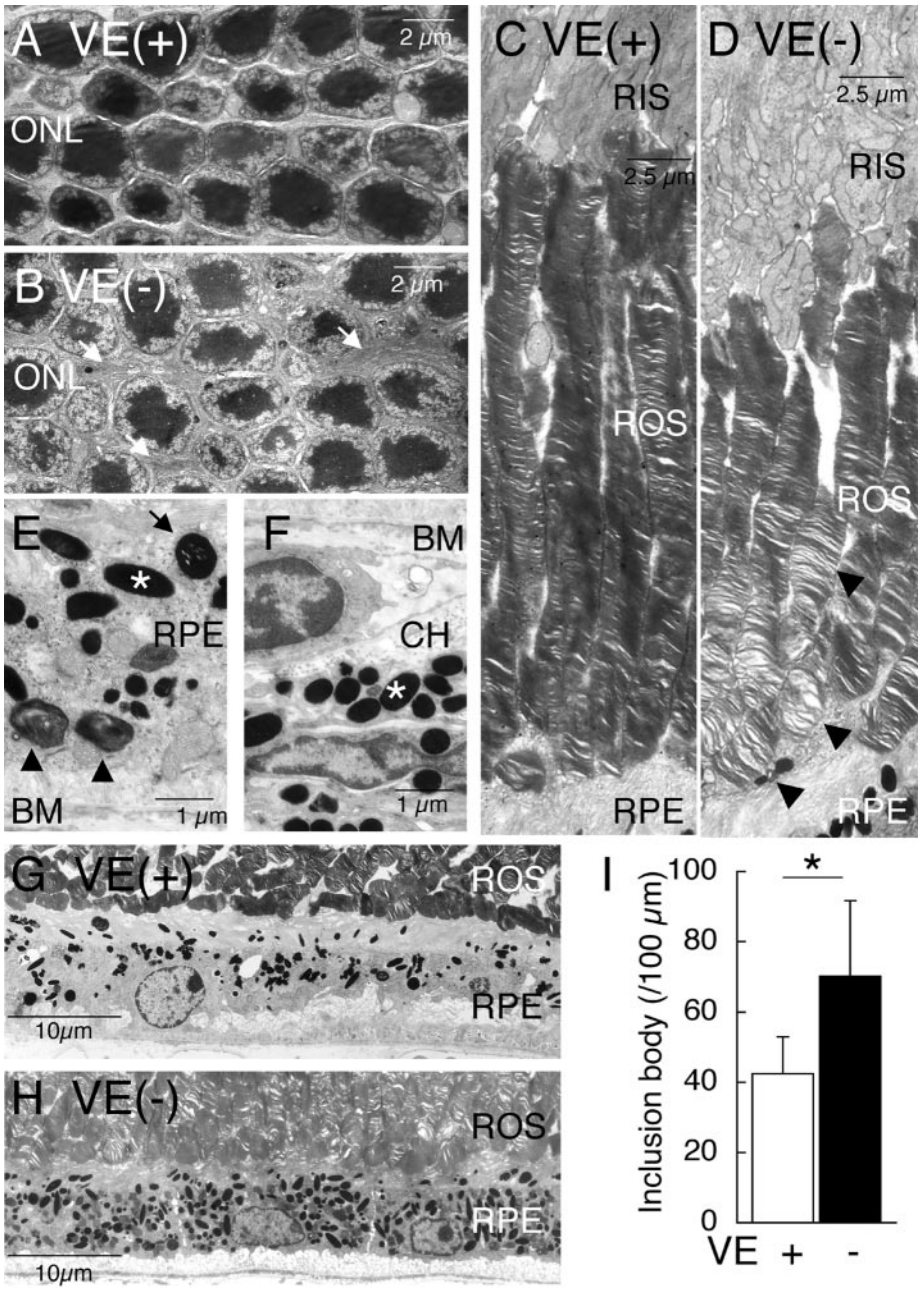

FIGURE 3. Ultrastructural observation by TEM. The eyes obtained from the 18-month-old mice belonging to the VE (+) group (four eyes from four mice) and the VE (−) group (six eyes from six mice) were analyzed. (**A, B**) Representative TEM images of the ONL in the VE (+; **A**) and VE (−; **B**) groups. Thick material was observed in the intercellular space of photoreceptor cell nuclei in the sections obtained from the VE (−) group (*arrow*). (**C, D**) Representative TEM images of the ROS in the VE (+; **C**) and VE (−; **D**) groups. The expanded and irregular arrangement of disc membranes was observed at the tip of the ROS in the sections obtained from the VE (−) group (arrowheads). (**E, F**) Representative TEM images of the inclusion bodies in the RPE (**E**) and the melanosomes in the RPE (**E**) and choroid (**F**). Inclusion bodies that contained whorls of electron-dense membranelike material (*arrowheads*) or contained more compressed and electron-dense material (arrows) were observed in the RPE cell bodies (**E**). These inclusion bodies were distinguishable from melanosomes (✶), which were the most electron dense, completely amorphous, and oval-shaped structures located in both the RPE (**E**) and choroid (**F**). (**G–I**) Representative TEM images of the RPE in the VE (+; **G**) and VE (−; **H**) groups, and the quantifications of the number of inclusion bodies (**I**). The data are expressed as the mean ± SD ($n = 4$ and 6 in the VE (+) and VE (−) groups, respectively). $^*P < 0.05$, as determined by an unpaired *t*-test. ONL, outer nuclear layer; RIS, rod inner segment; ROS, rod outer segment; RPE, retinal pigment epithelium; BM, Bruch's membrane; and CH, choroid.

Thickening of Bruch's membrane and formation of vacuoles in the RPE layer were observed in some sections; however, no consistent difference in the thickening and in the vacuole formations was observed between the VE (−) and the VE (+) groups.

Detection of Autofluorescence in the Retina

We assessed autofluorescence in the retinal sections obtained from the 4-month-old animals (Fig. 4). An autofluorescence signal of greater intensity was observed in the RPE layer of the VE (−) group (Fig. 4B, arrows) than in that of the VE (+) group (Fig. 4A).

tHODE and 8-iso-PGF$_{2\alpha}$ Levels in the Retina and RPE Fraction

Because oxidative stress is thought to be closely related to the aging process, we finally tested the levels of oxidative stress

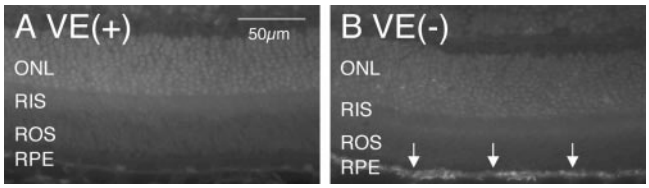

FIGURE 4. Detection of autofluorescence by using a fluorescence microscope. The eyes obtained from the 4-month-old mice belonging to the VE (+) group (two eyes from two mice) and the VE (−) group (two eyes from two mice) were analyzed. (**A, B**) Representative fluorescent images of the retinal sections obtained from the VE (+; **A**) and VE (−; **B**) groups. Remarkable autofluorescence is consistently observed in the RPE layer in the VE (−) group (*arrows*).

Table 3. Levels of HODE and isoPs in Retina and RPE Fraction from 4- and 18-Month-Old Animals

	4-Month Old								
	Retina			RPE Fraction			Retina + RPE Fraction		
	VE(+)	VE(−)	Ratio [VE(−)/(+)]	VE(+)	VE(−)	Ratio [VE(−)/(+)]	VE(+)	VE(−)	Ratio [VE(−)/(+)]
9,13-(*Z,E*) HODE	70 ± 30	36 ± 12	0.5	65 ± 11	67 ± 7	1.0	135 ± 26	104 ± 17	0.8
Ratio (18-mo/4-mo)									
9-(*E,E*) HODE	27 ± 14	17 ± 2	0.6	24 ± 4	38 ± 9	1.6*	51 ± 12	54 ± 9	1.1
Ratio (18-mo/4-mo)									
13-(*E,E*) HODE	29 ± 9	17 ± 6	0.6	104 ± 86	55 ± 16	0.5	133 ± 90	73 ± 21	0.6
Ratio (18-mo/4-mo)									
Total HODE	126 ± 51	71 ± 17	0.6	193 ± 92	160 ± 29	0.8	319 ± 119	231 ± 43	0.7
Ratio (18-mo/4-mo)									
8-iso-PGF2α	ND	0.2 ± 0.3	—	1.7 ± 0.3	2.5 ± 0.7	1.5	1.7 ± 0.3	2.7 ± 0.6	2.1*
Ratio (18-mo/4-mo)									

Values are expressed as the mean ± SD (picomoles/mg protein); $n = 4$ in 4-month-olds VE(+) and VE(−) and 18-month-old VE(+); $n = 6$ in 18-month-olds VE(−). ND, not detectable.

* $P < 0.05$ between VE(+) and VE(−) calculated by unpaired *t*-test.

†, ††, and ††† $P < 0.05$, < 0.01, and < 0.001, respectively, between 4- and 18-month-olds, by unpaired *t*-test.

markers such as tHODE and 8-iso-$PGF_{2\alpha}$ in the retinas and RPE fractions obtained from the 4- and 18-month-old animals (Table 3). On the one hand, in the 4-month-old animals, there was no significant difference between the VE (+) and VE (−) groups with regard to the tHODE levels in any of the tissues examined. On the other hand, 8-iso-$PGF_{2\alpha}$ was detected only in the retinas obtained from the VE (−) group (Table 3, 4-month-old). The 8-iso-$PGF_{2\alpha}$ level in the retina and RPE fraction was 2.1-fold higher in the VE (−) group than in the VE (+) group, and the difference was found to be significant ($P < 0.05$). The tHODE and 8-iso-$PGF_{2\alpha}$ levels in most tissues in the 18-month-old animals were higher than those in the tissues of the 4-month-old animals in both VE (−) and VE (+) groups. However, the increases related to aging were more remarkable in the VE (−) group (2.6- to 12.4-fold increase in HODE and 3.5- to 43.5-fold increase in 8-iso-$PGF_{2\alpha}$) than in the VE (+) group (0.8- to 7.3-fold increase in tHODE and 3.3- to 8.7-fold increase in 8-iso-$PGF_{2\alpha}$; Table 3, 18-month-old, ratio, 18 months/4 months). In the 18-month-old animals, the total HODE and 9,13-(Z,E) HODE levels in the retina and RPE fraction were significantly higher in the VE (−) group than in the VE (+) group, whereas there was no significant difference in the 9-(E, E) and 13-(E, E) HODE levels between the VE (−) and VE (+) groups.

Discussion

In the present study, the α-Toc levels in the VE (−) group markedly decreased in all the ocular tissues that were analyzed when compared to those in the VE (+) group (Table 1). In the retinas obtained from the VE (−) group, the α-Toc level was 71-fold lower than those obtained from the VE (+) group, indicating a more severe VE deficiency in dietary deprivation than ever reported.[19–21] Thus, severe VE deficiency achieved by the combined use of *a-TTP*$^{-/-}$ mice and a VE-deficient diet is thought to be an excellent model to assess the role of VE in vivo, particularly in tissues such as the retina that are resistant to the dietary deprivation of VE. Of interest, α-Toc deprivation was accompanied with a marked reduction in the γ-Toc level in the ocular tissues (Table 1). This finding is in agreement with our previous observation that the γ-Toc level in the plasma and liver decreased in the VE (−) group when compared to the VE (+) group.[36] Orally administered α- and γ-Tocs are equally absorbed from the intestine, but only α-Toc is preferentially secreted from the liver to the plasma, owing to its specific binding to α-TTP that is expressed in the liver.[37] The decreased γ-Toc level in the VE (−) group may suggest that α-TTP or α-Toc play a role in the uptake, retention, and metabolism of γ-Toc; however, this assumption must be confirmed. In the present study, we used wild-type C57BL/6 mice as the VE (+) control group. Any retinal phenotype of mice derived from the ES cell line used for the generation of *a-TTP*$^{-/-}$ mice was not reported, and *a-TTP*$^{-/-}$ mice used in the present study were backcrossed with C57BL/6 mice. Accordingly, we believe that the findings observed in the present study are due to the difference in tissue levels of VE between VE (+) and (−) groups and/or the elimination of *a-TTP* gene in VE (−) group.

Previous studies reported that the decrease in docosahexaenoic acid is a common feature of retinal disease, including hereditary[33,34] and light-induced[38] retinal degeneration. In the present study, *n*-3 PUFAs, including docosahexaenoic acid, decreased in the retinas and RPE fractions obtained from the VE (−) group when compared to the VE (+) group; thus, the concentration of other kinds of fatty acids remained unchanged or increased (Table 2). The dietary deprivation of VE and selenium in rats for 26–32 weeks led to a marked decrease in the concentration of *n*-3 PUFAs in the RPE fraction, but not in the whole retina,[20] which suggests that retinal degeneration observed in the present study was more severe than that observed in a previously reported experiment on dietary deficiency alone. Light microscopy revealed a significant decrease in the number of ONL nuclei in the VE (−) group when compared to that in the VE (+) group, whereas no significant difference was observed in the ONL thickness between the groups (Fig. 2). The presence of dense matrix between the ONL nuclei in the VE (+) group, as revealed by TEM (Fig. 3B),

TABLE 3 (*continued*). Levels of HODE and isoPs in Retina and RPE Fraction from 4- and 18-Month-Old Animals

18-Month-old								
Retina			RPE Fraction			Retina + RPE Fraction		
VE(+)	VE(−)	Ratio [VE(−)/(+)]	VE(+)	VE(−)	Ratio [VE(−)/(+)]	VE(+)	VE(−)	Ratio [VE(−)/(+)]
150 ± 61	435 ± 345	2.9	432 ± 377	828 ± 443	1.9	582 ± 428	1264 ± 373	2.2*
2.1	12.1		6.7	12.4††		4.3	12.2†††	
197 ± 150	199 ± 76	1.0	84 ± 64	156 ± 100	1.9	281 ± 150	355 ± 148	1.3
7.3	11.7††		3.5	4.1†		5.5†	6.6††	
65 ± 43	136 ± 115	2.1	78 ± 67	142 ± 78	1.8	142 ± 101	278 ± 135	2.0
2.2	8.0		0.8	2.6		1.1	3.8†	
411 ± 206	770 ± 514	1.9	594 ± 506	1127 ± 562	1.9	1006 ± 573	1896 ± 589	1.9*
3.3†	10.8†		3.1	7.0††		3.2	8.2†††	
9.2 ± 9.5	8.7 ± 7.0	1.0	5.6 ± 4.4	8.7 ± 2.9	1.6	14.8 ± 11.9	17.3 ± 9.3	1.2
—	43.5†		3.3	3.5††		8.7	6.4†	

explains this discrepancy. Recently, neural remodeling in retinal degeneration has been recognized, and the Müller cell hypertrophy plays an important role in such neural remodeling.[35,39,40] Müller cell hypertrophy is indicated by somatic translocation of Müller cells in the direction of the outer retina and by filling with Müller cell processes in intercellular space of the ONL.[35,39,40] Accordingly, compensatory hypertrophy of Müller cells is likely to be involved in the morphologic changes observed in the ONL of the VE (−) group. Previously, Yokota et al.[41] reported a change in the retinal morphology in *a-TTP*$^{-/-}$ mice. Although they did not perform quantification, they provided representative images of hematoxylin/eosin-stained retinal sections in their reports, showing that at the age of 20 months, the ONL thickness in the *a-TTP*$^{-/-}$ mice that were fed a normal diet was roughly half that in the wild-type mice fed a normal diet.[41] The reason for this discrepancy between the report published by Yokota et al. and the present study is not clear, but the difference in the light intensity in the vivarium or a small difference in the genetic background may have affected the phenotype.

TEM revealed a marked alteration in the ultrastructure of the ROS (Fig. 3D) and an accumulation of inclusion bodies in the RPE of the retinas obtained from the VE (−) group (Figs. 3H, 3I). These observations agreed with previous reports that aging alters the structure of the ROS and causes the accumulation of inclusion bodies in the RPE and that the deficiency of antioxidant nutrients, including VE, accelerates these retinal changes with aging.[19,25] Fluorescence microscopy revealed an accumulation of autofluorescence in the RPE obtained from the VE (−) group (Fig. 4B). Autofluorescent lipofuscin granules, which are indicative of inclusion bodies in the RPE, are thought to be an end product of lipid peroxidation; thus, oxidative stress is proposed to be involved in the age-related changes in the retina.[26,42] When the observations of the 18-month-old animals were compared to those of the 4-month-old animals, the tHODE and 8-iso-$PGF_{2\alpha}$ levels, which are biomarkers for lipid peroxidation, were found to be increased in the retinas and RPE fractions obtained from both VE (−) and VE (+) groups; however, these age-related increases were more remarkable in the VE (−) group (2.6- to 43.5-fold) than in the VE (+) group (0.8- to 8.7-fold; Table 3). Accordingly, our results support the previously proposed theory regarding the involvement of nonenzymatic oxidation of lipids in the retina and RPE in the aging process. It is known that the isomer distribution of HODE depends on the oxidants and antioxidants.[43] The racemic 9(*RS*)-(*E,E*)- and 13(*RS*)-(*E,E*)-HODE, which are formed in equal amounts, are markers for the free radical–meditated lipid peroxidation, although it does not clarify which radical initiated the chain oxidation. The regio-, stereo-, and enantio-specific product 13(*S*)-(*Z,E*)-HODE clearly indicates oxidation by 15-lipoxygenase, whereas 10- and 12-HODE indicate oxidation by singlet oxygen. The reason that (*Z,E*) and (*E,E*)-HODE showed different trends of change related to aging in this study (Table 3) should be investigated in the near future from the viewpoint of isomer distributions. Recently, we reported that the increase in tHODE and 8-iso-$PGF_{2\alpha}$ in retinal degeneration occurred after exposure to light in mice.[27] In the current study, we demonstrated the successful measurement of both oxidation products even in small amounts of the sample (i.e., one retinal sample [roughly 10 mg wet weight] in each measurement). Because the increase in both oxidation products was accompanied with retinal degeneration in this study, tHODE and 8-iso-$PGF_{2\alpha}$ can be said to be effective biomarkers for assessing age-related changes in the retina as well.

In summary, the combined use of *a-TTP*$^{-/-}$ mice and a VE-deficient diet leads to a severe deficiency of VE, enhances lipid peroxidation in the retina, and accelerates degenerative damage of the retina with age.

Acknowledgments

The authors thank Hiroyuki Arai at the University of Tokyo, Graduate School of Pharmaceutical Sciences for the development of *a-TTP*$^{-/-}$ mice; Mieko Hayakawa, Yoko Habuchi, and Nanako Itoh from the Human Stress Signal Research Center (HSSRC), the National Institute of Advanced Industrial Science and Technology (AIST) for excellent technical support.

References

1. Halliwell B, Gutteridge JMC. *Free Radicals in Biology and Medicine*. 3rd ed. Oxford, UK: Oxford University Press; 1999.
2. Niki E, Yoshida Y, Saito Y, Noguchi N. Lipid peroxidation: mechanisms, inhibition, and biological effects. *Biochem Biophys Res Commun*. 2005;338:668–676.
3. Winkler BS, Boulton ME, Gottsch JD, Sternberg P. Oxidative damage and age-related macular degeneration. *Mol Vis*. 1999;5:32.
4. Beatty S, Koh H, Phil M, Henson D, Boulton M. The role of oxidative stress in the pathogenesis of age-related macular degeneration. *Surv Ophthalmol*. 2000;45:115–134.
5. Lou MF. Redox regulation in the lens. *Prog Retin Eye Res*. 2003; 22:657–682.
6. Ganea E, Harding JJ. Glutathione-related enzymes and the eye. *Curr Eye Res*. 2006;31:1–11.
7. Tanito M, Kwon YW, Kondo N, et al. Cytoprotective effects of geranylgeranylacetone against retinal photooxidative damage. *J Neurosci*. 2005;25:2396–2404.
8. A randomized, placebo-controlled, clinical trial of high-dose supplementation with vitamins C and E, beta carotene, and zinc for age-related macular degeneration and vision loss: AREDS report no. 8. *Arch Ophthalmol*. 2001;119:1417–1436.
9. Bursell SE, Clermont AC, Aiello LP, et al. High-dose vitamin E supplementation normalizes retinal blood flow and creatinine clearance in patients with type 1 diabetes. *Diabetes Care*. 1999; 22:1245–1251.
10. Johnson L, Quinn GE, Abbasi S, Gerdes J, Bowen FW, Bhutani V. Severe retinopathy of prematurity in infants with birth weights less than 1250 grams: incidence and outcome of treatment with pharmacologic serum levels of vitamin E in addition to cryotherapy from 1985 to 1991. *J Pediatr*. 1995;127:632–639.
11. Pasantes-Morales H, Quiroz H, Quesada O. Treatment with taurine, diltiazem, and vitamin E retards the progressive visual field reduction in retinitis pigmentosa: a 3-year follow-up study. *Metab Brain Dis*. 2002;17:183–197.
12. van Rooij J, Schwartzenberg SG, Mulder PG, Baarsma SG. Oral vitamins C and E as additional treatment in patients with acute anterior uveitis: a randomised double masked study in 145 patients. *Br J Ophthalmol*. 1999;83:1277–1282.
13. Jacques PF, Taylor A, Moeller S, et al. Long-term nutrient intake and 5-year change in nuclear lens opacities. *Arch Ophthalmol*. 2005;123:517–526.
14. Packer L, Weber SU, Rimbach G. Molecular aspects of alpha-tocotrienol antioxidant action and cell signalling. *J Nutr*. 2001;131: 369S–73S.
15. Tanito M, Itoh N, Yoshida Y, Hayakawa M, Ohira A, Niki E. Distribution of tocopherols and tocotrienols to rat ocular tissues after topical ophthalmic administration. *Lipids*. 2004;39:469–474.
16. Arita M, Nomura K, Arai H, Inoue K. alpha-Tocopherol transfer protein stimulates the secretion of alpha-tocopherol from a cultured liver cell line through a brefeldin A-insensitive pathway. *Proc Natl Acad Sci USA*. 1997;94:12437–12441.
17. Ouahchi K, Arita M, Kayden H, et al. Ataxia with isolated vitamin E deficiency is caused by mutations in the alpha-tocopherol transfer protein. *Nat Genet*. 1995;9:141–145.
18. Gotoda T, Arita M, Arai H, et al. Adult-onset spinocerebellar dysfunction caused by a mutation in the gene for the alpha-tocopherol-transfer protein. *N Engl J Med*. 1995;333:1313–1318.
19. Katz ML, Stone WL, Dratz EA. Fluorescent pigment accumulation in retinal pigment epithelium of antioxidant-deficient rats. *Invest Ophthalmol Vis Sci*. 1978;17:1049–1058.
20. Farnsworth CC, Stone WL, Dratz EA. Effects of vitamin E and selenium deficiency on the fatty acid composition of rat retinal tissues. *Biochim Biophys Acta*. 1979;552:281–293.
21. Stephens RJ, Negi DS, Short SM, van Kuijk FJ, Dratz EA, Thomas DW. Vitamin E distribution in ocular tissues following long-term dietary depletion and supplementation as determined by microdissection and gas chromatography-mass spectrometry. *Exp Eye Res*. 1988;47:237–245.
22. Jishage K, Arita M, Igarashi K, et al. Alpha-tocopherol transfer protein is important for the normal development of placental labyrinthine trophoblasts in mice. *J Biol Chem*. 2001;276:1669–1672.
23. Yoshida Y, Itoh N, Hayakawa M, et al. Lipid peroxidation in mice fed a choline-deficient diet as evaluated by total hydroxyoctadecadienoic acid. *Nutrition*. 2006;22:303–311.
24. Katz ML, Eldred GE. Failure of vitamin E to protect the retina against damage resulting from bright cyclic light exposure. *Invest Ophthalmol Vis Sci*. 1989;30:29–36.
25. Katz ML, Parker KR, Handelman GJ, Bramel TL, Dratz EA. Effects of antioxidant nutrient deficiency on the retina and retinal pigment epithelium of albino rats: a light and electron microscopic study. *Exp Eye Res*. 1982;34:339–369.
26. Farnsworth CC, Dratz EA. Oxidative damage of retinal rod outer segment membranes and the role of vitamin E. *Biochim Biophys Acta*. 1976;443:556–570.
27. Tanito M, Yoshida Y, Kaidzu S, Ohira A, Niki E. Detection of lipid peroxidation in light-exposed mouse retina assessed by oxidative stress markers, total hydroxyoctadecadienoic acid and 8-iso-prostaglandin F(2alpha). *Neurosci Lett*. 2006;398:63–68.
28. Yoshida Y, Niki E. Detection of lipid peroxidation in vivo: total hydroxyoctadecadienoic acid and 7-hydroxycholesterol as oxidative stress marker. *Free Radic Res*. 2004;38:787–794.
29. Tanito M, Elliott MH, Kotake Y, Anderson RE. Protein modifications by 4-hydroxynonenal and 4-hydroxyhexenal in light-exposed rat retina. *Invest Ophthalmol Vis Sci*. 2005;46:3859–3868.
30. Tanito M, Masutani H, Kim YC, Nishikawa M, Ohira A, Yodoi J. Sulforaphane induces thioredoxin through the antioxidant-responsive element and attenuates retinal light damage in mice. *Invest Ophthalmol Vis Sci*. 2005;46:979–987.
31. Ohira A, Tanito M, Kaidzu S, Kondo T. Glutathione peroxidase induced in rat retinas to counteract photic injury. *Invest Ophthalmol Vis Sci*. 2003;44:1230–1236.
32. Forrest GL, Futterman S. Age-related changes in the retinal capillaries and the fatty acid composition of retinal tissue of normal and essential fatty acid-deficient rats. *Invest Ophthalmol*. 1972;11: 760–764.
33. Scott BL, Reddy TS, Bazan NG. Docosahexaenoate metabolism and fatty-acid composition in developing retinas of normal and rd mutant mice. *Exp Eye Res*. 1987;44:101–113.
34. Martin RE, Ranchon-Cole I, Brush RS, et al. P23H and S334ter opsin mutations: increasing photoreceptor outer segment n-3 fatty acid content does not affect the course of retinal degeneration. *Mol Vis*. 2004;10:199–207.
35. Marc RE, Jones BW, Watt CB, Strettoi E. Neural remodeling in retinal degeneration. *Prog Retin Eye Res*. 2003;22:607–655.
36. Yoshida Y, Itoh N, Hayakawa M, et al. Lipid peroxidation induced by carbon tetrachloride and its inhibition by antioxidant as evaluated by an oxidative stress marker, HODE. *Toxicol Appl Pharmacol*. 2005;208:87–97.
37. Kaempf-Rotzoll DE, Traber MG, Arai H. Vitamin E and transfer proteins. *Curr Opin Lipidol*. 2003;14:249–254.
38. Wiegand RD, Joel CD, Rapp LM, Nielsen JC, Maude MB, Anderson RE. Polyunsaturated fatty acids and vitamin E in rat rod outer segments during light damage. *Invest Ophthalmol Vis Sci*. 1986; 27:727–733.
39. Jones BW, Watt CB, Frederick JM, et al. Retinal remodeling triggered by photoreceptor degenerations. *J Comp Neurol*. 2003;464: 1–16.
40. Linberg KA, Fariss RN, Heckenlively JR, Farber DB, Fisher SK. Morphological characterization of the retinal degeneration in three strains of mice carrying the rd-3 mutation. *Vis Neurosci*. 2005;22: 721–734.
41. Yokota T, Igarashi K, Uchihara T, et al. Delayed-onset ataxia in mice lacking alpha-tocopherol transfer protein: model for neuronal degeneration caused by chronic oxidative stress. *Proc Natl Acad Sci USA*. 2001;98:15185–15190.
42. Hiramitsu T, Armstrong D. Preventive effect of antioxidants on lipid peroxidation in the retina. *Ophthalmic Res*. 1991;23:196–203.
43. Noguchi N, Yamashita H, Hamahara J, Nakamura A, Kuhn H, Niki E. The specificity of lipoxygenase-catalyzed lipid peroxidation and the effects of radical-scavenging antioxidants. *Biol Chem*. 2002; 383:619–626.